ASEAN Engineering Journal

Full Paper

SYNTHESIS AND CHARACTERIZATION OF BIMETALLIC MOF HKUST-1(CU, MG) ADSORBENTS AND THEIR APPLICATION IN NATURAL GAS PURIFICATION

Asmat Ullah Khan[a], Mohd Hafiz Dzarfan Othman[a]*, Mohammad Younas[b], Mohd Hafiz Puteh[a,c], Mukhlis A Rahman[a], Juhana Jaafar[a]

[a]Advance Membrane Technology Research Center (AMTEC), Faculty of Chemical and Energy Engineering, Universiti Teknologi Malaysia, 81310 UTM Johor Bahru, Malaysia
[b]Department of Chemical Engineering, Faculty of Mechanical, Chemical and Industrial Engineering, University of Engineering and Technology, Peshawar, Pakistan
[c]Faculty of Civil Engineering, Universiti Teknologi Malaysia, 81310 UTM Johor Bahru, Malaysia

Article history
Received
12 October 2023
Received in revised form
23 January 2024
Accepted
25 January 2024

*Corresponding author
hafiz@petroleum.utm.my

Graphical abstract

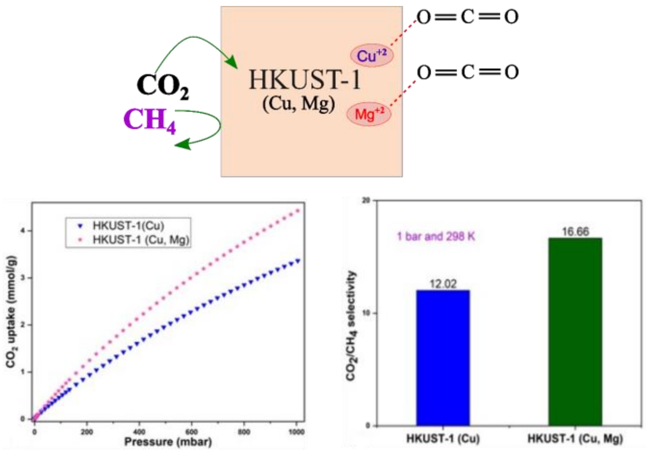

Abstract

Carbon dioxide (CO_2) is one of the most important greenhouse gases and its removal from natural gas by adsorption is highly desirable. This study investigates the synthesis process of the bimetallic metal-organic framework, HKUST-1(Cu, Mg) and its potential use in natural gas purification by preferentially adsorbing CO_2 from CO_2/CH_4 mixture. HKUST-1(Cu, Mg) was prepared by solvothermal method at different temperatures (100-200 °C). The resulting MOFs were characterized by various analytical techniques (XRD, SEM, FTIR, and TGA). The experimental results showed that single metal MOF HKUST-1 can be prepared at 100 °C, whereas the bimetallic HKUST-1(Cu, Mg) can be prepared by raising the temperature to 180 °C. Furthermore, the synthesized single and bimetallic MOFs were studied for their CO_2/CH_4 separation performance. The sorption results showed that the partial substitution of Cu metal with Mg metal in the framework of bimetallic HKUST-1(Cu, Mg) enhanced the CO_2 uptake and its selectivity over CH_4 by 31.7%, and 38.60%, respectively, which can be attributed to changes in surface areas, pore structures and additional open metal site (OMS) induced by the secondary metal. These findings shed light on the optimal synthesis conditions and highlight the CO_2 separation efficiency of HKUST-1(Cu, Mg) in natural gas upgrading.

Keywords: Bimetallic metal-organic framework, CO_2 adsorption, CO_2/CH_4 selectivity, Natural gas.

1.0 INTRODUCTION

Natural gas is considered a clean fuel because of low emissions as compared to oil and coal [1]. Natural gas sources can have up to 30% carbon dioxide (CO_2) by volume which can lead to a series of potential issues [2]. Gaseous CO_2 is a major contributor to the accumulation of greenhouse gases. Capturing CO_2 from natural gas is critical for environmental, economic, and operational reasons [3]. CO_2 capture improves the energy content and marketability of natural gas, lowers transportation costs, and can even create additional revenue streams if the captured CO_2 is used in other applications such as enhanced oil recovery. Reducing CO_2 content prevents the formation of hydrates that can clog pipelines and reduces corrosion risks to infrastructure [4].

To date, various technologies have been identified for post-combustion CO_2 capture, including pressure swing adsorption (PSA) [5], amine scrubbing [6], and membrane-based separation [7]. In PSA technique, high pressure is applied to adsorb CO_2 on solid adsorbents e.g., zeolites. The adsorption efficiency of zeolites is high, but since they are hydrophilic by nature and the gas stream contains water vapours that adsorb on the zeolite surface and consequently reduce the surface area available for CO_2 adsorption. Although amine scrubbing is the most widely used method for CO2 capture, it has a disadvantage due to the high regeneration cost of the solvent. In recent decades, membrane technology has made advances and developments in gas separation, but the process still needs to be optimized and the membrane material should be modified so that it can be used for commercial purposes [8]. Some of the above technologies have demonstrated promising separation performance, but high energy consumption and cost limit their use [9]. Therefore, there is a need for more environmentally sustainable and cost-effective alternative technologies for CO_2 capture.

Solid adsorbents such as mesoporous silica, zeolites, carbon nanocomposites, and metal-organic frameworks (MOFs) have shown promising results in selective adsorption of different gases due to their structural diversity and compositions [10, 11]. However, only a limited number of them possess the required properties for exceptional CO_2 adsorption separation [12, 13]. Among these materials, MOFs are considered an attractive option due to their large surface area, tunable porosity, and specific CO_2 binding sites [14-16].

In low- pressure situations such as atmospheric pressure, the weak interactions between the active sites and CO_2 molecules reduce the ability of MOFs to effectively capture CO_2 [17]. Therefore, various techniques have been investigated to enhance the CO_2 adsorption performance of MOFs, such as functionalization [18], metal insertion [19], cation exchange [20], framework interpenetration [21], and metal ions substitution in MOFs [22]. The strategy of “metal ion substitution” is considered as a useful tool for modifying MOF structures, allowing the creation of bimetallic MOFs either by direct synthesis or by post-synthetic modification (PSM) [23]. Bimetallic MOFs, i.e., MOFs composed of two different metal ions, have been investigated as potential material for CO_2 capture from flue gas. There is a limited literature on CO_2 adsorption studies using bimetallic MOFs.

The addition of a secondary metal ion in MOFs has the potential to increase the stability of MOFs and improve the MOF-CO_2 interaction [24]. For instant, Cui et al. [25] synthesized hybrid bimetallic frameworks using metal ion exchange strategy by partially replacing Zn^{+2} ions in Zn-1 [Zn_3(L)2(dabco)(H_2O)]-9DMF, with Cu^{+2} ions to prepare bimetallic Zn-1’. The newly synthesized bimetallic Zn-1’ showed improved N_2 adsorption and high stability compared to the monometallic Zn-1. Similarly, He et al. [26] used a microdroplet spray method for the synthesis of bimetallic MOFs, including Cu-BTC(Fe), Cu-BTC(Mg), Cu-BTC(Co), and Cu-BTC(Al), by replacing the Cu metal in the starting MOF with iron (Fe), Mg, cobalt (Co), and aluminum (Al), respectively. Their results showed that the incorporation of a small quantity of dopant metal ions into the framework did not damage the crystalline structure. Instead, it led to an increase in BET surface area, which can be attributed to the expansion of the unit cell caused by the substitution of the metal ions. The bi-metallic MOF showed enhanced gas adsorption performance, which can be explained by different electrostatic interactions between the secondary metal ions and the gas molecules. Zhang et al. [27] added Mg metal into Cu-BTC@MWCNT composite adsorbents to enhance CO_2 adsorption from syngas. The Mg-doped composite showed up to 3.7% improvement in CO_2 adsorption capacity compared to pure Cu-BTC. This improved CO_2 adsorption can be attributed to the high affinity of alkali metal (Mg) and acidic CO_2 molecules. In another study, Wang et al. [28] successfully prepared bimetallic MOFs in a single step reaction by incorporating zinc (Zn) metal into the Cu-based HKUST-1 MOF. The maximum percentage of Cu^{+2} metal replaced by Zn^{+2} in the paddle wheel units was up to 21%. However, the observed N_2 adsorption capacity and specific surface areas of the bimetallic Cu_3-xZnx$(BTC)_2$ MOFs decreased with increasing Zn^{+2}/Cu^{+2} molar ratio. However, in-depth studies on synthesis and application of bimetallic MOFs for CO2 adsorption from raw natural gas are still lacking.

This study investigates the CO_2 and CH_4 adsorption on HKUST-1(Cu) and bi-metallic HKUST-1(Cu, Mg) at 273 and 298 K, using a volumetric apparatus. Cu metal in the representative MOF, HKUST-1 was partially substituted with Mg metal to synthesized bimetallic MOF. Systematic characterization were performed to confirm the secondary metal ion substitution and study the structure and morphology of the modified MOF adsorbents. The bimetallic MOF retained its original crystalline structure after the incorporation of secondry metal. CO_2 and CH_4 sorption measurements were performed and the effects of the secondary metal sites on CO_2 adsorption and CO_2/CH_4 selectivity were analysed. Overall, the present work will highlight the effect of secondary metal sites on the selective adsorption of CO_2 from natural gas by bimetallic MOFs.

2.0 EXPERIMENTAL SECTION

2.1 Materials

All the chemicals used in this study were analytical grade and were used without any further purification. Copper nitrate trihydrate (Cu $(NO_3)_2{\cdot}3H_2O$, 98%), magnesium nitrate hexahydrate (Mg $(NO_3)_2{\cdot}6H_2O$, 98%), and 1,3,5-benzenetricarboxylic acid (H_3BTC, 99%) were purchased from Sigma-Aldrich. Methanol (MeOH), ethanol (EtOH), dimethyl formamide (DMF), and deionized (DI) water were purchased from Elite Advanced Materials. Nitrogen (CH_4, ≥ 99.5%) and Carbon dioxide (CO_2, ≥ 99.995%) were purchased from Alpha Gas Solution Malaysia.

2.2 Synthesis of HKUST-1 and bimetallic HKUST-1(Cu, Mg)

In this study, we synthesized HKUST-1(Cu) using a solvothermal technique, reported by Chowdhury et al. [16]. In a typical experiment, first Copper (II) nitrate trihydrate (6 mmol) was dissolved in 12 ml of deionized water. In another flask, H_3BTC (4 mmol) was dissolved in 24 ml of a 1:1 mixture of ethanol and DMF. The two solutions were then mixed and magnetically stirred at ambient temperature for 30 minutes. The reaction mixture was transferred into a 100-ml PPL-lined stainless-steel autoclave and subjected to heat at 100°C for 10 hours. After the reaction ended, the autoclave was allowed to cool to room temperature. The resulting blue crystals were separated using a centrifuge at a speed of 3000 rpm for 15 minutes. To remove the unreacted H_3BTC and metal salts, the synthesized material was rinsed thrice with DMF until neutral pH. The crystals were then immersed in MeOH for 3 days, with an exchange of fresh solvent after each 4 h. Finally, the crystals were activated at 120 °C for 4 h to remove the residual solvents. Figure 1 illustrates the schematic of the synthesis scheme used to prepare the bimetallic HKUST-1(Cu, Mg).

Bi-metallic HKUST-1 (Cu, Mg) was synthesized by in situ metal substitution and one-pot hydrothermal method following the procedure reported in the literature [29]. For the synthesis bimetallic MOF, Copper (II) nitrate trihydrate (8 mmol) and Magnesium (II) nitrate hexahydrate (1 mmol) was dissolved in 16 ml DI water. The remaining procedure was similar to that of the parent HKUST-1 (Cu), with the only difference being an increase in the reaction temperature from 100 to 200 oC.

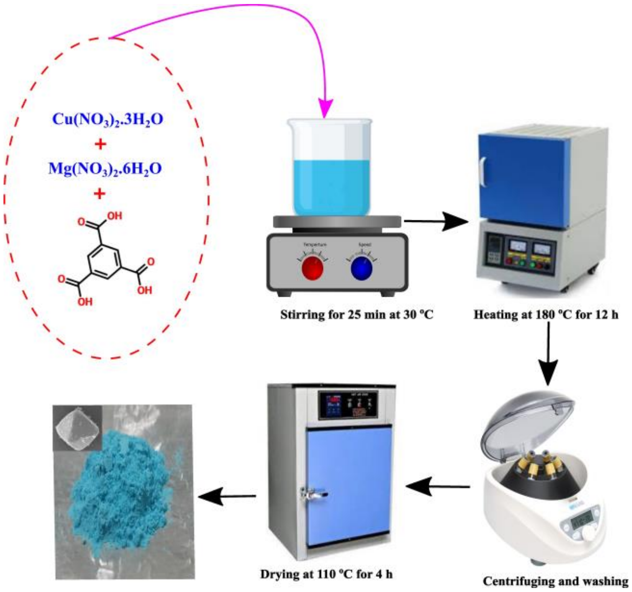

Figure 1 Schematic of synthesis scheme used to prepare bimetallic HKUST-1(Cu, Mg) MOF.

2.3 Characterizations

Various analytical techniques were used to characterize the MOF powder. FE-SEM was used to study surface morphology, and EDX provided elemental composition details. PXRD confirmed the crystal structure and phase purity. FTIR was employed to investigate the chemical bonds and functional groups in HKUST-1(Cu) and Bi-metallic HKUST-1(Cu, Mg). ICP-OES quantified Copper and Magnesium levels before and after the reaction. For evaluating surface properties, N_2 adsorption-desorption tests were conducted at 77 K, and specific surface areas were computed using the BET method. Pore volume and size were estimated through BJH method at a relative pressure of P/P0 = 0.99. The TGA was performed to assess the thermal stability of the samples.

2.4 Adsorption theory of ideal solution IAST

Ideal Adsorbed Solution Theory (IAST) is a predictive model that does not require any mixture data. In gas purification and separation procedures, IAST serves as a tool for predicting the equilibrium and selectivity of multicomponent adsorption, relying exclusively on experimental single-component adsorption isotherms. It is a thermodynamic approach in which the adsorbed phase is assumed to form an ideal solution that satisfies Raoult's law for vapour-liquid equilibrium [30]. The ideal CO_2/CH_4 selectivity of component a over b is given by.

$$s_{ab} = \frac{x_a/x_b}{y_a/y_b} \text{....} (1)$$

where x_a and y_a represent mole fractions of component “a” in the adsorbed phase and in gas phase respectively, while x_b and y_b represent mole fractions of component “b” in the adsorbed and gas phases respectively. The single component adsorption isotherms have been fitted to the following dual site Langmuir-Freundlich (DSLF) model to enable the application of the IAST calculation [31].

$$y = \frac{k1k2x^{k3}}{1+k2x^{k3}} + \frac{l1l2x^{l3}}{1+l2x^{l3}} \text{....(2)}$$

where Y is the amount adsorbed in mmol/g, X is the pressure in bar, k_1 and l_1 are the saturation capacities in mmol/g, k_2 and l_2 are the Langmuir parameter in bar-1 and k_3 and l_3 are the Freundlich parameter for dual sites 1 and 2 respectively.

2.5 Isosteric Heat of CO_2 Adsorption

The isosteric heat of adsorption (Qst) is an important thermodynamic measure that indicates the amount of heat either released or absorbed during the adsorption process. This value can be derived from adsorption isotherms recorded at minimum two different temperatures [32]. The amount of gas adsorbed to the adsorbent surface is affected by factors such as temperature, pressure, and isosteric heat of adsorption. For gas separation, an intermediate Qst value is desirable for specific adsorbent-adsorbate pairs. This is because too low Qst value results in weak gas adsorption, while an extremely high Qst value increases the cost of adsorbent regeneration [33]. The Qst values in this study were calculated from the CO_2 adsorption isotherm at 273.15 k and 298 K using the linear version of the Clausius–Clapeyron equation [34].

$$Q_{st} = RT_1T_2 \frac{\ln{(P_1/P_2)}}{T_2-T_1} \text{.... (3)}$$

where, Q_{st} is the isosteric heat of adsorption (KJ/mol), T_1, T_2 is the temperature (K), and P_1, P_2 is pressure (mbar) of measurement, and R is the universal gas constant (8.314 J/mol/K).

3.0 RESULTS AND DISCUSSION

3.1 Material properties of HKUST-1 and bimetallic HKUST-1 (Cu, Mg)

The morphologies of the single and bimetallic MOF samples were studied at FE-SEM as shown in Figure 2(a & b). The as-synthesized HKUST-1 sample in Figure 2(a) showed an octahedral morphology which is in accordance with the structure reported in the literature [35, 36]. The bimetallic HKUST-1(Cu, Mg) sample shown in Figure 2(b) also exhibited the same octahedral morphology as that of the parent MOF, indicating that doping with a secondary metal does not change the octahedral morphology of the MOF. The average particle size of the MOF sample was about 10–20 µm, which is consistent with the literature [37]. It can be seen in Figure 2 (a & b) that Mg metal doping does not have any effect on particle size. The EDS analysis was performed to confirm the presence of Mg metal in the HKUST-1(Cu, Mg) bimetallic samples. Figure 2(c) displays the EDS spectra of HKUST-1(Cu, Mg) confirming the coexistence of both metals Cu and Mg in the bimetallic MOF sample.

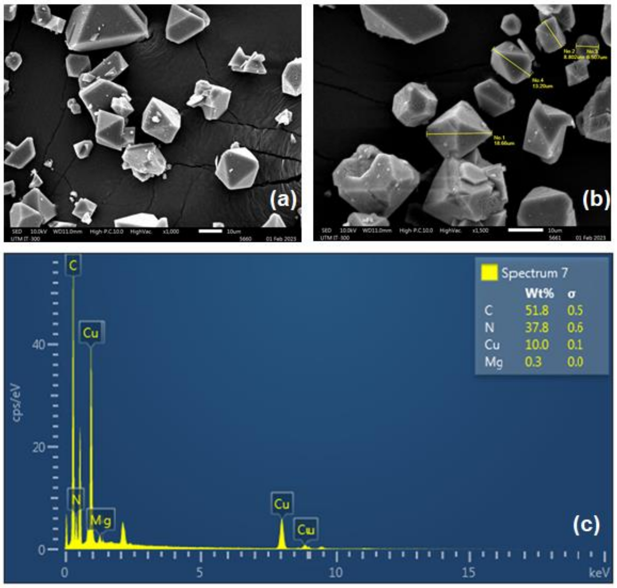

Figure 2. (a & b) FE-SEM micrograph; (a) HKUST-1(Cu), (b) HKUST-1(Cu, Mg), and (c) EDX spectrum of HKUST-1(Cu, Mg).

In order to investigate the phase purity and crystalline structure of MOF adsorbents, the XRD analysis was performed. Figure 3(a) shows the XRD patterns of single and bimetallic MOF adsorbents. The XRD diffraction pattern of the HKUST-1(Cu) shows the predominant peaks at 2θ= 6.70, 9.40, 11.60, 13.30, 17.40, 19.10, 25.80 and 29.40 that are in accordance with published data [38-40]. The Mg-doped bimetallic HKUST-1(Cu, Mg) showed similar diffraction patterns to the parent MOF, suggesting that the crystal structure was well preserved.

Figure 3(b) displays the FT-IR spectra of bimetallic MOF adsorbents. Obviously, pure HKUST-1(Cu) and bimetallic HKUST-1(Cu, Mg) have the similar infrared spectra in agreement to that reported in the previous literature [39], indicating that they are formed by the same building block, the benzene-1,3,5-tricarboxylate (BTC) linker. The bands observed at 760 and 730 cm^{-1} were attributed to the substitution of Cu for the hydrogen atom on the benzene ring, while the band at 1110 cm^{-1} corresponded to the stretching vibration of C-O-Cu. The band observed around 1715 cm^{-1} were ascribed to the acidic C=O stretching vibration in BTC which is shifted to 1643 cm^{-1} after complexation with Cu^{+2} [41].

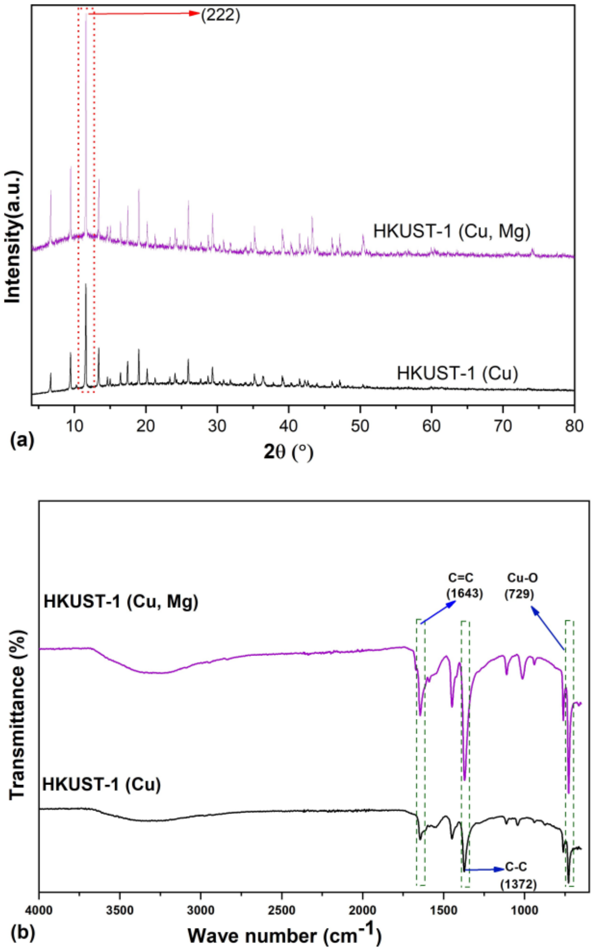

Figure 3 Structural characterization of MOF samples. (a) XRD patterns and (b) FT-IR spectra.

Figure 4 (a) shows the N_2 adsorption isotherms of HKUST-1 and bimetallic HKUST-1 (Cu, Mg) MOFs at 77 K. The curves distribution were mainly type-I and in good agreement to that reported in the literature [42]. Notably, the curves extends sharply at low pressure region and then enhances slowly while remaining almost flat, indicating that the materials had abundance of micropores. It is clear from Figure 4 that the N_2 uptake and BET surface area (SBET) of the resulting bimetallic MOF changes with the incorporation of Mg metal. For the HKUST-1 sample, the N_2 uptake and SBET were 15 (mmol/g) and 1198 (m^2/g) at 1 bar and 77K, respectively. For the bimetallic HKUST-1 (Cu, Mg) sample, the N_2 adsorption capacity and SBET were found to be 22.20 (mmol/g) and 1580 (m^2/g), showing an increasing trend in both N_2 adsorption and SBET. These findings are consistent with the literature [43].

Textural properties of MOF-199(Cu, Mg) samples are shown in Table 1.

TGA analysis was performed to study the thermal stability of MOF samples at 800 ◦C under N_2 atmosphere. Figure 5 shows the thermograms of pure HKUST-1 and bimetallic HKUST-1 (Cu, Mg) adsorbents. Three stages in decomposition of both samples were observed, which were in accordance to the results reported in literature [44]. The small weight loss (6.6%) between 42 and 122 °C can be ascribed to the removal of adsorbed water. The weight loss (15%) between 122 and 330 0C was due to the evaporation of coordinated DMF molecules from the adsorbent Structure. In final step, the curve showed a prominent weight loss (40%) between 330 and 450 °C, which can be ascribed to the decomposition of the benzene tricarboxylate linker and the collapse of the framework. The single and bimetallic MOF adsorbents showed similar thermograms, indicating that the incorporation of Mg metal does not change the thermal stability.

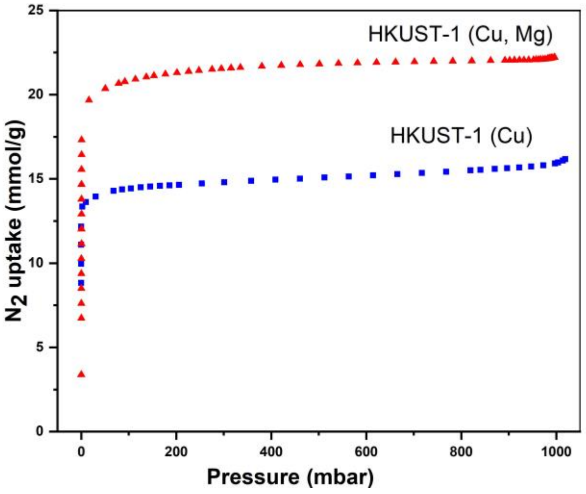

Figure 4 N_2 adsorption isotherms Of MOF adsorbents at 77 K

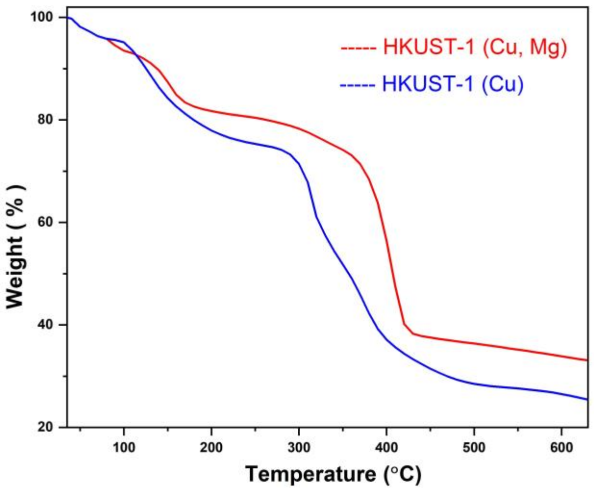

Figure 5 TGA curves of MOF adsorbents

Table 1 Textural properties of PEI-functionalized MOF-199(Cu, Mg) samples

MOFs	S_{BET} (m^2/g)	Langmuir Surface area (m^2/g)	Pore Volume (cm^3/g)	Average pore size (nm)	Crystal size (nm)
HKUST-1 (Cu)	1198	1,495	0.5152	7.0341	85.05
HKUST-1 (Cu, Mg)	1580	2,153	0.7725	2.9143	141.6

3.2 Adsorption performance of HKUST-1 and bimetallic HKUST-1 (Cu, Mg)

The gas adsorption efficiency of the as-prepared MOF adsorbents were investigated at different temperatures and pressures. Figure 5(a) displays the CO_2 adsorption isotherms at 1 bar and 273.15 K. The single metal MOF HKUST-1 showed a CO_2 adsorption capacity of 7.31 (mmol/g). Partially substituting Cu with Mg metal in bimetallic HKUST-1(Cu, Mg) sample exhibited a CO_2 uptake of 8.61 (mmol/g) at 1 bar, higher than most of the reported MOF-based adsorbents [43]. The observed enhancement in S_{BET} and gas uptake can be ascribed to stronger electrostatic interaction between the open metal sites (OMS) of Mg atom and CO_2 molecules [45]. The following Table 2 shows the characteristics of CO_2 and CH_4 gases.

Table 2 Characteristics of CO_2 and CH_4 gases [46].

Gas	Polarizability ($\times 10^{-25}$ cm^3)	Dipole moment ($\times 10^{18}$ esu cm)	Quadrupole moment ($\times 10^{-26}$ esu cm^2)
CO_2	26.5	0.00	4.30
CH_4	26.0	0.00	0.00

The CO_2 adsorption performance of HKUST-1 and bimetallic HKUST-1 (Cu, Mg) at 298 k and 1 bar are shown in Figure 5(b). The CO_2 uptake of both samples was observed to be decreased with increase in temperature. When the temperature was increased from 273.15 K to 298 K, the CO_2 adsorption of parent MOF reduced from 7.31 to 3.36 (mmol/g), while for the bimetallic HKUST-1 (Cu, Mg), the CO_2 adsorption reduced from 8.61 to 4.42 (mmol/g). This decrease in CO_2 adsorption can be ascribed to physical adsorption as the predominant mechanism for CO_2 capture in these adsorbents [47]. The Figure 5(c) displays the CH4 adsorption isotherms of parent MOF and modified bimetallic MOF adsorbents at 298 k. The single metal MOF HKUST-1 showed a CH_4 uptake of 0.28 (mmol/g) and the bimetallic HKUST-1 (Cu, Mg) showed a CH_4 uptake of 0.26 (mmol/g) at 1 bar and 298 K.

IAST has been widely used to predict the adsorption selectivity of gas mixtures using single gas isotherms. In the present study, IAST was used to predict the CO_2 selectivity of a binary CO_2/CH_4 mixture. The DSLF equation was used to fit a single-component isotherm. At the same temperature and pressure, both HKUST-1 and HKUST-1 (Cu, Mg) samples showed significantly lower CH_4 uptake compared to CO_2 uptake. The higher CO_2 adsorption can be attributed to the higher polarizability of CO_2, the higher quadrupole moment, and the smaller kinetic diameter. [48]. Figure 5(d) shows the ideal CO_2/Ch_4 selectivity of HKUST-1 and bimetallic HKUST-1 (Cu, Mg) samples determined using natural gas compositions (CO_2/CH_4: 50/50). HKUST-1 (Cu) exhibited an ideal CO_2/CH_4 selectivity of 12.02, similar to the value reported in the literature [49]. The bimetallic HKUST-1 (Cu, Mg) exhibited a higher selectivity of 16.66, corresponding to an increase of 38.60% after Mg metal doping. This enhancement in CO_2 selectivity can be attributed to the stronger electrostatic interaction between the OMSs of Mg metal and CO_2 molecule [36].

The isosteric heat of adsorption is one of the most important indicators for measuring the adsorption strength of the adsorbent [50]. Figure 5(e) displays the isosteric heat of CO_2 adsorption on the HKUST-1(Cu, Mg) bimetallic sample as a function of the amount of CO_2 adsorbed. As shown in Figure 5(e), the Qst values increase from 23.70 to 28.69 (kJ/mol) with the increase of gas adsorption during the process. This range of Qst values indicates that the process is physical adsorption. This increasing trend in Qst is unusual [51, 52], and indicates the possible formation of CO_2 clusters in the pores of the adsorbent [53]. Similar trends have been reported in the literature for other MOFs [54]. The mutual attraction between the CO_2 molecules in the pores of the MOF might have increased with the increase of the adsorption amount, leading to an increased isosteric heat of adsorption [55].

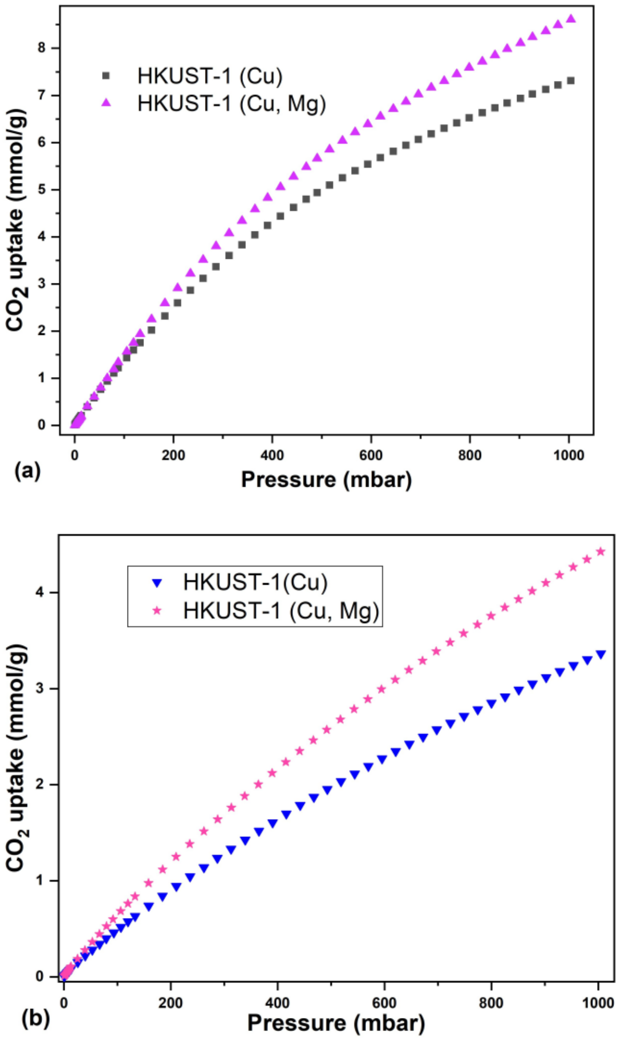

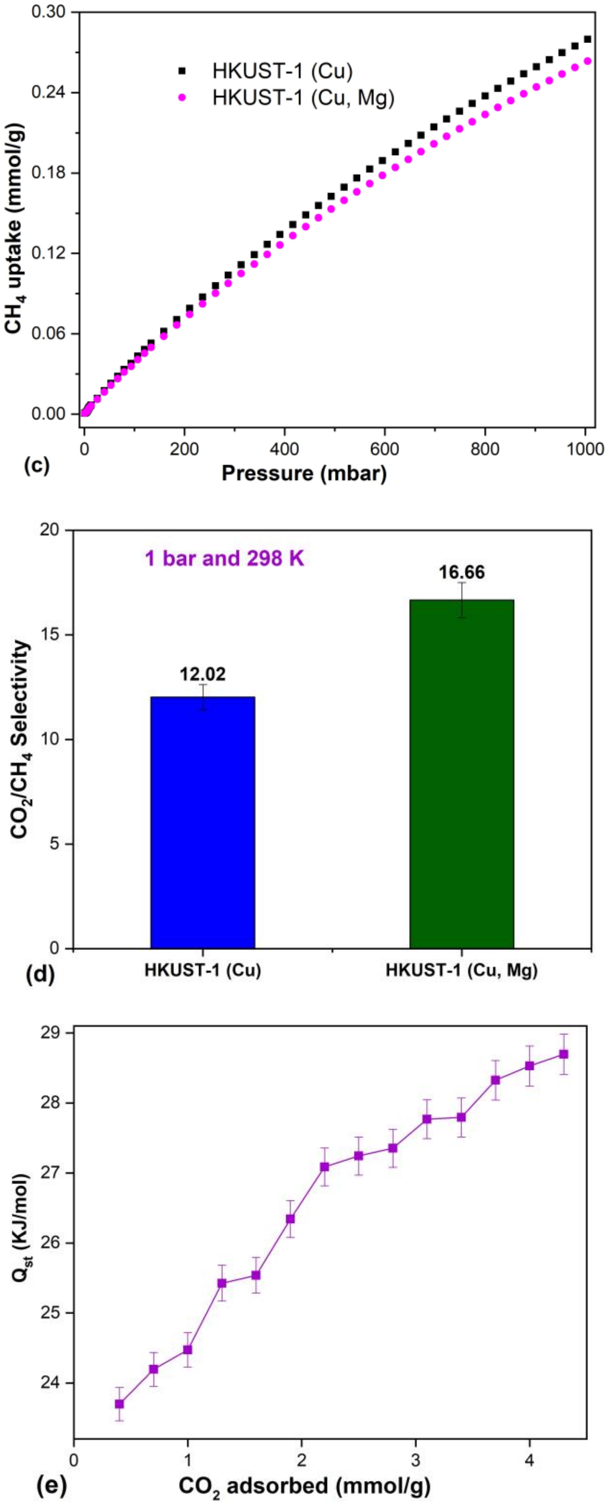

Figure 5. Adsorption performance of bimetallic MOF adsorbents. (a) CO_2 adsorption isotherms at 273.15K, (b) CO_2 adsorption isotherms at 298 K, (c) CH_4 adsorption isotherms at 298 K, (d) Selectivity of HKUST-1 and bimetallic HKUST-1(Cu, Mg) for CO_2/CH_4, and (D) Isosteric heat of adsorption for HKUST-1(Cu, Mg).

4.0 CONCLUSION

In the study, the single-metal MOF HKUST-1(Cu) and bimetallic MOF HKUST-1(Cu, Mg) was successfully synthesized by a solvothermal method at different temperatures. It was found that the single-metal MOF HKUST-1 can be synthesized at 100 °C, while a temperature of 180 °C is required for the synthesis of its bimetallic counterpart. Several analytical techniques, such as XRD, SEM, FTIR, TGA, and BET were used to characterize the MOF adsorbents. The study focusses on the application of these MOFs in separation of CO_2 from CH_4. The results showed that the partial substitution of Cu with Mg in bimetallic MOF improved the CO_2 uptake and selectivity over CH_4 by 31.7% and 38.6%, respectively. These improvements can be ascribed to changes in surface areas, pore structures, and additional open metal sites created by the secondary metal (Mg). Notably, the substitution of the secondary metal did not affect the crystalline structure of the parent MOF.

Acknowledgement

The authors express their sincere gratitude to the Ministry of Higher Education for the support received under the Science and Technology Research Partnership for Sustainable Development (SATREPS) scheme (Vote number: R.J130000.7809.4L97 and Universiti Teknologi Malaysia under High Impact Research (UTM-HIR) (Vote number: Q.J130000.2409.08G34) and Fundamental Research (UTMFR) (Vot number: Q.J130000.3809.22H07). Acknowledgments are also extended to the Research Management Centre and Advanced Membrane Technology Research Centre at Universiti Teknologi Malaysia for their financial and technical assistance.

Conflicts of Interest

The author(s) declare(s) that there is no conflict of interest regarding the publication of this paper

References

[1] Chong ZR, Yang SHB, Babu P, Linga P, Li X-S. 2016. Review of natural gas hydrates as an energy resource: Prospects and challenges. *Applied Energy*.162:1633-52.

[2] Iarikov DD, Oyama ST. 2011. Review of CO2/CH4 separation membranes. *Membrane science and technology.* 14: 91-115. Elsevier.

[3] Ullah A, Shah MUH, Ahmed J, Younas M, Othman MHD. 2022 Ionic Liquids and Metal-Organic Frameworks as Advanced Environmental Materials for CO2 Capture. *Handbook of Energy Materials.* 1-29. Springer.

[4] Shen J, Wang X, Chen Y. 2023. Adsorbents for adsorption separation of CO2 and CH4: A literature review. *The Canadian Journal of Chemical Engineering*.101(12): 7115-33.

[5] Riboldi L, Bolland O. 2016. Pressure swing adsorption for coproduction of power and ultrapure H2 in an IGCC plant with CO2 capture. *International Journal of Hydrogen Energy*.41(25): 10646-60.

[6] Abdeen FR, Mel M, Jami MS, Ihsan SI, Ismail AF. 2016. A review of chemical absorption of carbon dioxide for biogas upgrading. *Chinese Journal of Chemical Engineering*.24(6): 693-702.

[7] Li S, Pyrzynski TJ, Klinghoffer NB, Tamale T, Zhong Y, Aderhold JL, et al. 2017. Scale-up of PEEK hollow fiber membrane contactor for post-combustion CO2 capture. *Journal of Membrane Science*.527: 92-101.

[8] Dai Z, Ansaloni L, Deng L. 2016. Recent advances in multi-layer composite polymeric membranes for CO2 separation: A review. *Green Energy & Environment*.1(2): 102-28.

[9] Bui M, Adjiman CS, Bardow A, Anthony EJ, Boston A, Brown S, et al. 2018. Carbon capture and storage (CCS): the way forward. *Energy & Environmental Science*.11(5): 1062-176.

[10] Yang B, Liu Y, Li M. 2016. Separation of CO2–N2 using zeolite NaKA with high selectivity. *Chinese Chemical Letters*.27(6): 933-7.

[11] Samuel O, Othman MHD, Kamaludin R, Dzinun H, Imtiaz A, Li T, et al. 2023. Photocatalytic degradation of recalcitrant aromatic hydrocarbon compounds in oilfield-produced water: A critical review. *Journal of Cleaner Production*. 137567.

[12] Jannatabadi AA, Bastani D, Norouzbahari S, Ghadimi A. 2021. CO2 and CH4 diffusivities through synthesized ZIF-8 nanocrystals: An experimental and theoretical investigation. *Microporous and Mesoporous Materials*.324: 111292.

[13] Qian Q, Asinger PA, Lee MJ, Han G, Mizrahi Rodriguez K, Lin S, et al. 2020. MOF-based membranes for gas separations. *Chemical reviews*.120(16): 8161-266.

[14] Karra JR, Walton KS. 2008. Effect of open metal sites on adsorption of polar and nonpolar molecules in metal− organic framework Cu-BTC. *Langmuir*.24(16): 8620-6.

[15] Wang T, Lin E, Peng Y-L, Chen Y, Cheng P, Zhang Z. 2020. Rational design and synthesis of ultramicroporous metal-organic frameworks for gas separation. *Coordination Chemistry Reviews*.423: 213485.

[16] Ali SA, Khan AU, Mulk WU, Khan H, Nasir Shah S, Zahid A, et al. 2023. An Ongoing Futuristic Career of Metal–Organic Frameworks and Ionic Liquids, A Magical Gateway to Capture CO2; A Critical Review. *Energy & Fuels*.37(20): 15394-428.

[17] Ullah S, Bustam MA, Al-Sehemi AG, Assiri MA, Kareem FAA, Mukhtar A, et al. 2020. Influence of post-synthetic graphene oxide (GO) functionalization on the selective CO2/CH4 adsorption behavior of MOF-200 at different temperatures; an experimental and adsorption isotherms study. *Microporous and Mesoporous Materials*.296: 110002.

[18] Wang B, Huang H, Lv X-L, Xie Y, Li M, Li J-R. 2014. Tuning CO2 selective adsorption over N2 and CH4 in UiO-67 analogues through ligand functionalization. *Inorganic chemistry*.53(17): 9254-9.

[19] Bloch ED, Britt D, Lee C, Doonan CJ, Uribe-Romo FJ, Furukawa H, et al. 2010. Metal insertion in a microporous metal− organic framework lined with 2, 2′-bipyridine. *Journal of the American Chemical Society*.132(41): 14382-4.

[20] An J, Rosi NL. 2010. Tuning MOF CO2 adsorption properties via cation exchange. *Journal of the American Chemical Society*.132(16): 5578-9.

[21] Nugent P, Belmabkhout Y, Burd SD, Cairns AJ, Luebke R, Forrest K, et al. 2013. Porous materials with optimal adsorption thermodynamics and kinetics for CO2 separation. *Nature*.495(7439): 80-4.

[22] Koh HS, Rana MK, Hwang J, Siegel DJ. 2013. Thermodynamic screening of metal-substituted MOFs for carbon capture. *Physical Chemistry Chemical Physics*.15(13): 4573-81.

[23] Yang X, Xu Q. 2017. Bimetallic metal–organic frameworks for gas storage and separation. *Crystal Growth & Design*.17(4): 1450-5.

[24] Chen L, Wang H-F, Li C, Xu Q. 2020. Bimetallic metal–organic frameworks and their derivatives. *Chemical science*.11(21): 5369-403.

[25] Cui P-P, Zhang X-D, Wang P, Zhao Y, Azam M, Al-Resayes SI, et al. 2017. Zinc (II) and copper (II) hybrid frameworks via metal-ion metathesis with enhanced gas uptake and photoluminescence properties. *Inorganic Chemistry*.56(22): 14157-63.

[26] He X, Chen D-R, Wang W-N. 2020. Bimetallic metal-organic frameworks (MOFs) synthesized using the spray method for tunable CO2 adsorption. Chemical Engineering Journal.382:122825.

[27] Zhang Y, Wibowo H, Zhong L, Horttanainen M, Wang Z, Yu C, et al. 2021. Cu-BTC-based composite adsorbents for selective adsorption of CO2 from syngas. *Separation and Purification Technology*.279: 119644.

[28] Wang T, Li X, Dai W, Fang Y, Huang H. 2015. Enhanced adsorption of dibenzothiophene with zinc/copper-based metal–organic frameworks. *Journal of Materials Chemistry A*.3(42): 21044-50.

[29] Gotthardt MA, Schoch R, Wolf S, Bauer M, Kleist W. 2015. Synthesis and characterization of bimetallic metal–organic framework Cu–Ru-BTC with HKUST-1 structure. *Dalton Transactions*.44(5): 2052-6.

[30] Walton KS, Sholl DS. 2015. Predicting multicomponent adsorption: 50 years of the ideal adsorbed solution theory. *AIChE Journal*.61(9): 2757-62.

[31] Bae Y-S, Farha OK, Spokoyny AM, Mirkin CA, Hupp JT, Snurr RQ. 2008. Carborane-based metal–organic frameworks as highly selective

sorbents for CO 2 over methane. *Chemical Communications.* (35): 4135-7.

[32] Ojeda-López R, Domínguez-Ortiz A, Felipe C, Cervantes-Uribe A, Pérez-Hermosillo IJ, Esparza-Schulz JM. 2021. Isosteric enthalpy behavior of CO2 adsorption on micro-mesoporous materials: carbon microfibers (CMFs), SBA-15, and amine-functionalized SBA-15. *Journal of Composites Science*.5(4): 102.

[33] An L, Liu S, Wang L, Wu J, Wu Z, Ma C, et al. 2019. Novel nitrogen-doped porous carbons derived from graphene for effective CO2 capture. *Industrial & Engineering Chemistry Research*.58(8): 3349-58.

[34] Amesimeku J, Zhao Y, Li K, Gu J. 2023. Rapid synthesis of hierarchical cerium-based metal organic frameworks for carbon dioxide adsorption and selectivity. *Microporous and Mesoporous Materials*. 112658.

[35] Aarti A, Bhadauria S, Nanoti A, Dasgupta S, Divekar S, Gupta P, et al. 2016. [Cu3 (BTC) 2]-polyethyleneimine: an efficient MOF composite for effective CO2separation. *RSC Advances*.6(95): 93003-9.

[36] Denning S, Majid AA, Lucero JM, Crawford JM, Carreon MA, Koh CA. 2020. Metal–organic framework HKUST-1 promotes methane hydrate formation for improved gas storage capacity. *ACS Applied Materials & Interfaces.*12(47):53510-8.

[37] Lin K-S, Adhikari AK, Ku C-N, Chiang C-L, Kuo H. 2012. Synthesis and characterization of porous HKUST-1 metal organic frameworks for hydrogen storage. I*nternational Journal Of Hydrogen Energy*. 37(18): 13865-71.

[38] Allmond K, Stone J, Harp S, Mujibur K. 2017. Synthesis and electrospraying of nanoscale MOF (metal organic framework) for high-performance CO 2 adsorption membrane. *Nanoscale research letters.*12:1-12.

[39] Vrtovec N, Mazaj M, Buscarino G, Terracina A, Agnello S, Arčon I, et al. 2020. Structural and CO2 Capture Properties of Ethylenediamine-Modified HKUST-1 Metal–Organic Framework. *Crystal Growth & Design*. 20(8): 5455-65.

[40] Goyal N, Kim J, Othman MR. 2023. Pentaethylenehexamine modified microporous MOF-199 for improved carbon dioxide uptake and enhanced carbon dioxide-nitrogen selectivity. *Microporous and Mesoporous Materials.*354: 112531.

[41] Sun X, Gu X, Xu W, Chen W-J, Xia Q, Pan X, et al. 2019. Novel hierarchical Fe (III)-doped Cu-MOFs with enhanced adsorption of benzene vapor. *Frontiers In Chemistry*.7: 652.

[42] Yan X, Hu X, Komarneni S. 2014. Facile synthesis of mesoporous MOF/silica composites. *RSC Advances.* 4(101): 57501-4.

[43] Ghanbari T, Abnisa F, Daud WMAW. 2020. A review on production of metal organic frameworks (MOF) for CO2 adsorption. *Science of The Total Environment*.707: 135090.

[44] Bodkhe GA, Hedau BS, Deshmukh MA, Patil HK, Shirsat SM, Phase DM, et al. 2020. Detection of Pb (II): Au Nanoparticle Incorporated CuBTC MOFs. *Frontiers in Chemistry*.8: 803.

[45] Bao Z, Yu L, Ren Q, Lu X, Deng S. 2011. Adsorption of CO2 and CH4 on a magnesium-based metal organic framework. *Journal Of Colloid And Interface Science.* 353(2): 549-56.

[46] Salehi S, Anbia M. 2017. High CO2 adsorption capacity and CO2/CH4 selectivity by nanocomposites of MOF-199. *Energy & Fuels*.31(5): 5376-84.

[47] Gan L, Andres-Garcia E, Mínguez Espallargas G, Planas JG. 2023. Adsorptive Separation of CO2 by a Hydrophobic Carborane-Based Metal–Organic Framework under Humid Conditions. *ACS Applied Materials & Interfaces.* 15(4): 5309-16.

[48] Abid HR, Rada ZH, Li Y, Mohammed HA, Wang Y, Wang S, et al. 2020. Boosting CO 2 adsorption and selectivity in metal–organic frameworks of MIL-96 (Al) via second metal Ca coordination. *RSC Advances*. 10(14): 8130-9.

[49] Zhang Y, Huang Y, Chen S, Shi L, Wang J, Yi Q, et al. 2023. In-situ construction of ionic ultramicroporous metal–organic frameworks for high-efficiency CO2/CH4 separation. *Chemical Engineering Journal.*471: 144580.

[50] Nuhnen A, Janiak C. 2020. A practical guide to calculate the isosteric heat/enthalpy of adsorption via adsorption isotherms in metal–organic frameworks, MOFs. Dalton Transactions.49(30):10295-307.

[51] Zhao X, Bu X, Nguyen ET, Zhai Q-G, Mao C, Feng P. 2016. Multivariable modular design of pore space partition. *Journal of the American Chemical Society*.138(46): 15102-5.

[52] Guo T, Ma N, Pan Y, Bedane AH, Xiao H, Eić M, et al. 2018. Characteristics of CO2 adsorption on biochar derived from biomass pyrolysis in molten salt. The Canadian *Journal of Chemical Engineering*. 96(11): 2352-60.

[53] Liang L, Liu C, Jiang F, Chen Q, Zhang L, Xue H, et al. 2017. Carbon dioxide capture and conversion by an acid-base resistant metal-organic framework. *Nature communications*.8(1): 1233.

[54] Qazvini OT, Babarao R, Telfer SG. 2021. Selective capture of carbon dioxide from hydrocarbons using a metal-organic framework. *Nature Communications.*12(1): 197.

[55] Zhou S, Wang H, Zhang P, Guo W. 2019. Investigation of the isosteric heat of adsorption for supercritical methane on shale under high pressure. *Adsorption Science & Technology.*37(7-8): 590-606.